

# Split & Merge: Unlocking the Potential of Visual Adapters via Sparse Training

Qizhe Zhang<sup>1</sup>   Bocheng Zou<sup>2</sup>   Ruichuan An<sup>3</sup>   Jiaming Liu<sup>1</sup>   Shanghang Zhang<sup>1†</sup>

<sup>1</sup>National Key Laboratory for Multimedia Information Processing, School of Computer Science, Peking University

<sup>2</sup>School of Computer Science and Technology, Xi'an Jiaotong University

<sup>3</sup>School of Software Engineering, Xi'an Jiaotong University

{theia, jiamingliu, shanghang}@pku.edu.cn

{bocheng.zou, arctanx}@stu.xjtu.edu.cn

## Abstract

With the rapid growth in the scale of pre-trained foundation models, parameter-efficient fine-tuning techniques have gained significant attention, among which Adapter Tuning is the most widely used. Despite achieving efficiency, Adapter Tuning still underperforms full fine-tuning, and the performance improves at the cost of an increase in parameters. Recent efforts address this issue by pruning the original adapters, but it also introduces training instability and suboptimal performance on certain datasets. Motivated by this, we propose *Mixture of Sparse Adapters*, or *MoSA*, as a novel Adapter Tuning method to fully unleash the potential of each parameter in the adapter. We first **split** the standard adapter into **multiple** non-overlapping modules, then stochastically activate modules for **sparse** training, and finally **merge** them to form a complete adapter after tuning. In this way, *MoSA* can achieve significantly better performance than standard adapters without any additional computational or storage overhead. Furthermore, we propose a hierarchical sparse strategy to better leverage limited training data. Extensive experiments on a series of 27 visual tasks demonstrate that *MoSA* consistently outperforms other Adapter Tuning methods as well as other baselines by a significant margin. Furthermore, in two challenging scenarios with low-resource and multi-task settings, *MoSA* achieves satisfactory results, further demonstrating the effectiveness of our design. Our code will be released.

## 1. Introduction

In computer vision, the *pre-training* paradigm has witnessed remarkable success [7, 22, 23]. Models pre-trained on large-scale datasets (e.g. ImageNet-21k [60], JFT-300M [62], SA-1B [32]) have demonstrated significant performance improvements across various downstream tasks. With pre-trained models, *transfer learning* aims

<sup>†</sup> Corresponding author. Code: <https://github.com/Theia-4869/MoSA>.

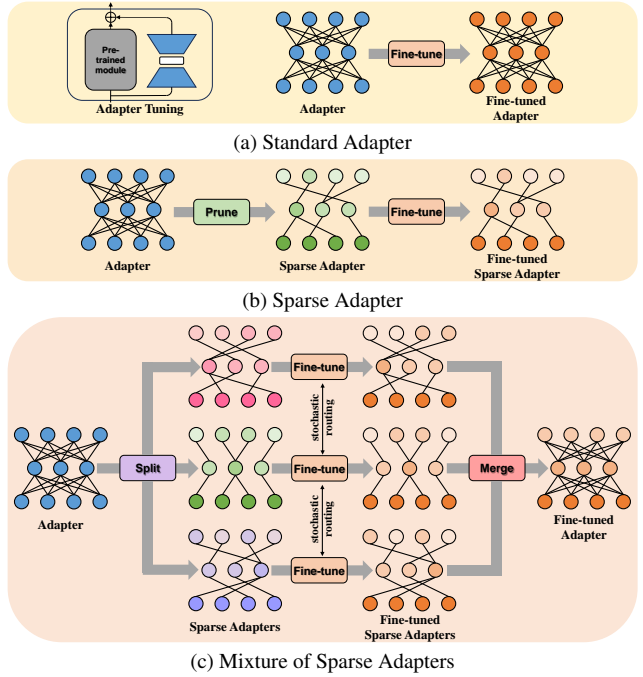


Figure 1. Different Adapter Tuning diagrams: (a) Adapter Tuning schema and standard adapter. (b) Sparse adapter. (c) Our proposed Mixture of Sparse Adapters (MoSA). We first split the standard adapter into multiple non-overlapping modules, then stochastically activate them for sparse training, and finally merge them to form a complete dense adapter.

to transfer the acquired knowledge to novel target domains, where labeled training samples are typically insufficient [3, 53, 79]. One of the most direct methods is *fine-tuning*, wherein pre-trained model parameters are further updated based on downstream task data [33, 71]. Currently, the widely adopted fine-tuning approach is full fine-tuning, involving the update of all parameters in the pre-trained model during tuning. However, as the scale of pre-trained models continues to escalate (e.g. ViT-G/14 [76] with over 1.8B parameters), storing the complete set of parameters

for each task becomes impractical, giving rise to the field of parameter-efficient fine-tuning (PEFT), which addresses this challenge by updating only a small subset of parameters from the pre-trained model for each downstream task. PEFT not only ensures the efficiency of parameter storage but also optimizes the utilization of available data.

Recently, various PEFT methods have emerged [27, 29, 37–39, 41, 74], with one of the most notable being *Adapter Tuning* [6, 8, 26, 52, 54, 57, 58]. This kind of method introduces additional lightweight modules to the pre-trained model while freezing the model backbone, achieving impressive results. Adapters [26, 57, 58] first make advancements in natural language processing. AdaptFormer [6], on the other hand, changes the adapter insertion form from sequential to parallel, achieving better results in ViT [13] architecture and visual tasks. Moreover, there is a growing trend in the visual domain towards adapters designed specifically for visual tasks [52, 54]. Despite the consideration for parameter efficiency, these adapters still underperform standard full fine-tuning. Increasing the bottleneck dimension in adapters can raise performance, but this comes at the cost of introducing too many additional parameters. Recent efforts have explored pruning the entire model [1, 19, 70] or adapter [24] before tuning to enhance the efficiency of parameter utilization, seemingly mitigating this problem to some extent. However, excessive sparsity can lead to instability and suboptimal performance on certain datasets. The delicate balance between parameter efficiency and performance remains a key challenge in Adapter Tuning methods.

In this paper, we propose *Mixture of Sparse Adapters (MoSA)* as a solution to the aforementioned issues, enhancing adapter performance without introducing additional computational and storage overhead. This is achieved through the incorporation of sparsity and mixture-of-expert (MoE) [59, 61, 78]. We start by splitting the standard adapter into several non-overlapping modules, each can be considered as a sparse adapter. Since the parameters of each module need to be updated, we employ a random way for decomposition, and experiments show that this approach is both concise and effective. During the training phase, to avoid extra computational costs, we use a non-routing stochastic activation mechanism. Each activated module uses a mask to filter gradients, achieving sparsity in parameter updates. We merge all sparse adapters into a complete dense adapter, achieving efficiency in both storage and computation during inference. Through this design, the potential of the original adapter structure is fully unleashed, maximizing the elimination of parameter redundancy.

Rather than simply stacking two independent approaches, our design organically integrates the sparse training with MoE, where the two components mutually reinforce each other. On one hand, the training process with mixed experts ensures expressive capability and stability

in downstream tasks, addressing the limitations of sparse training. On the other hand, sparse update of parameters more efficiently utilizes training data, alleviating the data dilution caused by sparse activation of multiple experts. To better facilitate the combination of the two components, we further propose a hierarchical sparse strategy. The dense down-projection layer provides robust intermediate features for the model, while multiple sparse up-projection layers increase the capacity of the model. It’s worth noting that our approach, as a general concept of enhancing parameter utilization, can be applied to various adapter structures and other addition-based PEFT methods. On 27 diverse downstream visual tasks with a pre-trained ViT backbone, our *MoSA* consistently outperforms all other fine-tuning methods, including full fine-tuning. Compared to full fine-tuning, *MoSA* achieves a lead of 1.36% (on FGVC), 2.43% (on VTAB) and 1.51% (on GICD), while updating only around 1% of the parameters compared to the pre-trained backbone. Compared to the standard adapter, *MoSA* achieves an improvement of 1.32% (on FGVC), 1.06% (on VTAB) and 0.36% (on GICD) without adding any computational or storage overhead. Additionally, we conducted comprehensive ablation experiments to validate the effectiveness of each component in our design.

We summarize our main contributions as follows:

- We propose a novel Adapter Tuning method, namely *MoSA*, for fully unleashing the potential of the standard adapters. Through a sparse and mixed training approach involving splitting and merging, our method maximizes parameter efficiency, enhancing the performance of Adapter Tuning in visual tasks.
- *MoSA* maximizes the balance between efficiency and performance. It exhibits efficiency in all the sparsification, mixed training, and inference, and the organic integration of sparsity and MoE further enhances performance.
- We evaluate our method on a total of 27 downstream visual tasks spanning different domains, and *MoSA* significantly outperforms full fine-tuning as well as all other PEFT baselines. In addition to common scenarios, *MoSA* also achieves optimal results in challenging scenarios such as low-resource and multi-task settings, further demonstrating the rationality of our design.

## 2. Related work

### 2.1. Parameter-efficient fine-tuning (PEFT)

Recently, many large-scale pre-trained models (*e.g.* LLaMA2 [63] 70B, GPT-3 [5] 175B) have emerged in deep learning research, which can achieve excellent performance in a variety of downstream tasks. However, updating and storing all model parameters for each downstream task has become far more expensive. PEFT achieves efficiency in training and storage by updating only a small fraction of

parameters compared to pre-trained models [27, 29, 30, 37–40, 42, 74], among which Adapter Tuning is one of the most widely used methods. Adapter [26] updates only the parameters of newly added lightweight bottleneck modules while freezing the model backbone during fine-tuning, achieving great success in NLP tasks. AdapterFusion [57] adjusts the position of the adapter and combines the parameters of adapters in multiple tasks to better adapt to multi-task scenarios. AdaptFormer [6] improves the performance of ViT [13] on visual tasks by changing the connection pattern of adapters from sequential to parallel. Moreover, ST-Adapter [52] and DualPath [54] use adapters to do image-to-video transfer learning. In contrast to the methods mentioned above, in this paper, we propose a new framework for training multiple sparse adapters, aiming to enhance performance while maintaining the efficiency of the original Adapter Tuning approach.

## 2.2. Mixture-of-experts (MoE)

The origin proposal of MoE [28] is targeted at enhancing model capacity. The earliest proposed technologies, known as soft MoE [47], integrate outputs of multiple experts through weighted summation. However, this technique significantly increases the computational cost during training. To address this issue, the sparsely-gated MoE [21, 61, 78] was introduced, selecting specific experts for activation and directly assigning data to them, thereby reducing the computational burden. Nonetheless, this method often resulted in load imbalance, with some experts becoming inactive in later training stages, risking system collapse. THOR [80] effectively mitigates this issue by implementing random activation, which not only enhances efficiency but also improves overall model performance. Unlike most previous methods in the fields, which typically employ the complete model as a singular expert encompassing all functionalities, our approach innovatively utilizes the sparse PEFT module as a distinct expert within the training process. After completing the training phase, we strategically combine these modules to form a cohesive and optimized system, which is pivotal for maximizing parameter efficiency, ensuring that our model not only maintains high performance but also operates with reduced computational demand.

## 2.3. Pruning and sparse training

The primary goal of model pruning [20, 46, 50] originally aimed to minimize deployment costs by reducing model parameters without significantly impacting its performance. Recent studies [1, 19, 70] have revealed that pruning can enhance model fine-tuning. A reduced number of trainable parameters can act as an additional regularization constraint, potentially improving performance. As a PEFT method, the architecture of adapters [26, 57] inherently possesses few updatable parameters. SparseAdapter [1] extends this con-

cept by pre-pruning the Adapter, enhancing parameter efficiency while maintaining or even improving performance compared to standard adapters. However, excessive sparsity can lead to training instability and suboptimal results on certain datasets. We take one step further to solve aforementioned weakness via integrating the MoE paradigm into our sparse tuning process. This integration not only achieves a sparse network structure, but also implements sparse activation during the training phase, which overcomes the inherent constraints of using a single sparse network.

## 3. Method

The adapter is a bottleneck form of PEFT module, where the standard adapter can enhance model capacity by increasing bottleneck dimensions at the cost of too many additional parameters. [24] achieves parameter efficiency through pre-pruning, but excessive sparsity can lead to instability and performance degradation. To achieve the optimal balance between efficiency and performance, we propose MoSA, which achieves efficiency through splitting and sparse training, while ensuring performance through stochastic activation and merging. To this end, we first overview our method in Sec. 3.1. Subsequently, we describe how we split the standard adapter into multiple sparse adapters in Sec. 3.2. Then, we introduce the training strategy with stochastic activation of multiple sparse experts in Sec. 3.3. Finally, in Sec. 3.4, we merge the split sparse adapters into a complete one for efficiency during inference.

### 3.1. Overview

Adapter Tuning is commonly employed in Transformer-based networks, which adapts the pre-trained representation to the target domain by injecting bottleneck modules into the Transformer layer. The general form of Adapter Tuning can be represented as:

$$\tilde{x} \leftarrow x + f(x \cdot \mathcal{W}^{\text{down}}) \cdot \mathcal{W}^{\text{up}} \quad (1)$$

where  $x \in \mathbb{R}^d$  represents the input of the adapter,  $f$  is the activation function, and  $\mathcal{W}^{\text{down}} \in \mathbb{R}^{d \times r}$  and  $\mathcal{W}^{\text{up}} \in \mathbb{R}^{r \times d}$  denote the linear layers for down-projection and up-projection, respectively.  $r$  is the bottleneck dimension, satisfying  $r \ll d$ , which allows for a reduction in the number of parameters in the adapter. [24] further exploits the high efficiency of parameters by pruning  $\mathcal{W}^{\text{down}}$  and  $\mathcal{W}^{\text{up}}$  before tuning. In our work, we split the standard adapter into  $N$  sparse adapters  $\mathcal{W}^{\text{down}} = \{\mathcal{W}_i^{\text{down}}\}_{i=1}^N$ ,  $\mathcal{W}^{\text{up}} = \{\mathcal{W}_i^{\text{up}}\}_{i=1}^N$ , and stochastically activate one of them during the training process for adaptation:

$$\tilde{x} \leftarrow x + f(x \cdot \mathcal{W}_i^{\text{down}}) \cdot \mathcal{W}_j^{\text{up}} \quad (2)$$

where  $i, j \in \{1, \dots, N\}$ , representing the stochastic selection of one from  $N$  sparse adapters. The overall design of our method is shown in Fig. 2.

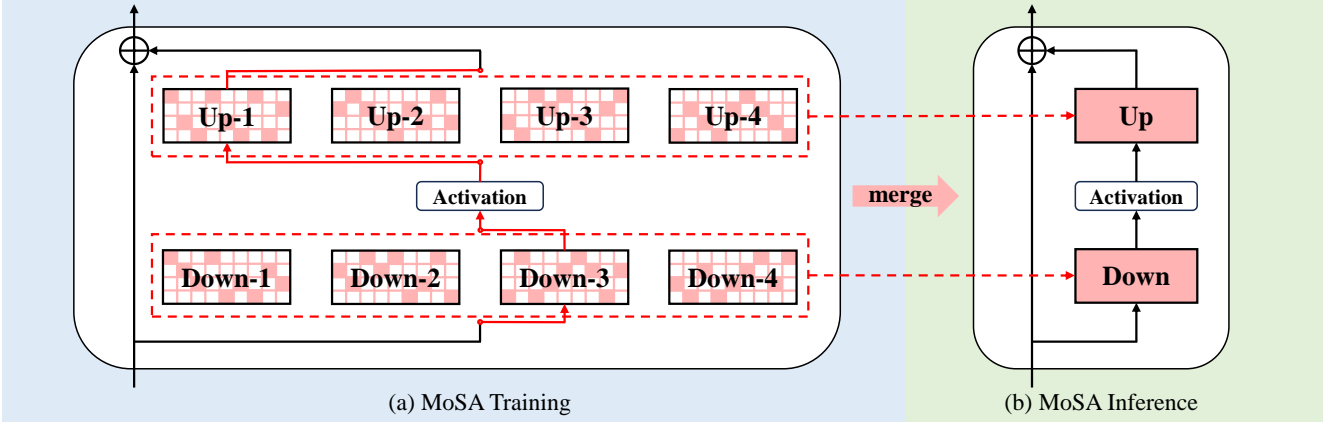


Figure 2. Architecture design of Mixture of Sparse Adapters. In the training phase, MoSA stochastically activates a sparse adapter during each forward pass; in the inference phase, MoSA merges multiple sparse adapters into a complete one to enhance inference efficiency.

### 3.2. Sparse adapter splitting

To make the most of all the parameters within a single adapter, we first split the standard adapter into multiple sparse adapters, as illustrated in Fig. 1. As all parameters in the adapter need to be updated, unlike [24], we do not adopt the task-specific pruning mechanism but instead employ a random splitting method to achieve as balanced grouping as possible, which also avoids the additional overhead of gradient computation based on downstream tasks before fine-tuning. Given the parameter of adapter  $\mathcal{W} \in \mathbb{R}^{d \times r}$ , we first generate an initial score  $\mathcal{S} \sim \text{Uniform}(0, 1) \in \mathbb{R}^{d \times r}$  for it. Then, we split  $\mathcal{W}$  into  $N$  non-overlapping sparse adapters  $\mathcal{W}_i : i \in \{1, \dots, N\}$ . Denoting the  $i$ -th  $N$ -quantile of all values in the matrix  $\mathcal{S}$  as  $s_i : i \in \{1, \dots, N\}$ , we obtain  $N$  sparse masks  $\mathcal{M}_i$  as follows:

$$\mathcal{M}_i \leftarrow \mathbb{I}[s_{i-1} \leq \mathcal{S} < s_i] \quad (3)$$

where  $\mathbb{I}$  represents an all-ones matrix, and  $s_0 = 0$ .

Once the masks are calculated, sparse gradient updating is performed according to the following form:

$$\mathcal{W}'_i \leftarrow \mathcal{W}_i + \varepsilon \nabla \mathcal{L}(\mathcal{W}_i) \odot \mathcal{M}_i \quad (4)$$

where  $\varepsilon$  represents the update step size, and  $\nabla \mathcal{L}(\mathcal{W}_i)$  denotes the gradient of the task loss with respect to  $\mathcal{W}_i$ . In this way, the positions with a mask value of 0 have their gradients filtered to 0, thereby freezing the corresponding parameters and achieving sparse training for the adapter.

### 3.3. Stochastic activation tuning

With multiple sparse adapters, each can be treated as an expert, allowing for mixed training. Traditional MoE methods [61, 78] involve a routing mechanism, introducing additional computation and load imbalance. Considering that Adapter Tuning itself serves as a parameter-efficient

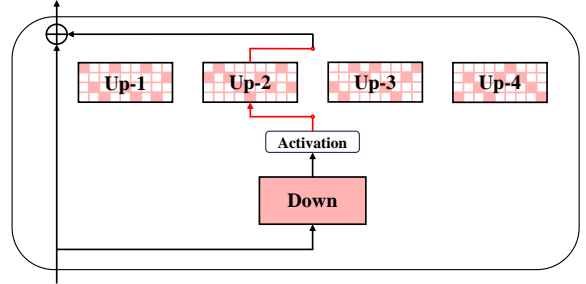


Figure 3. Hierarchical Mixture of Sparse Adapters. We preserve the down-projection layer in the adapter as a dense matrix, while only applying sparse splitting to the up-projection layer.

method, and inspired by [68, 80], in the training process of MoSA, we also adopt a completely stochastic activation mechanism, which has been demonstrated to be simple yet effective in the following experiments. Given two partitioned parameter sets  $\mathcal{W}^{\text{down}}$  and  $\mathcal{W}^{\text{up}}$ , for each batch of data, we randomly sample one module  $\mathcal{W}_i^{\text{down}} \in \mathcal{W}^{\text{down}}$ ,  $\mathcal{W}_j^{\text{up}} \in \mathcal{W}^{\text{up}}$  from each set to form an adapter  $\mathcal{W} = \{\mathcal{W}_i^{\text{down}}, \mathcal{W}_j^{\text{up}}\}$ , as shown in Eq. (2). This activation mechanism ensures consistency in parameters and computational load with standard Adapter Tuning during the training process. Additionally, activating different sparse modules each time enables the model to learn different representations, thereby increasing the model capacity.

**Hierarchical sparse strategy.** Although the MoE system enhances the model capacity, the sparse activation also reduces the amount of data seen by individual experts, resulting in suboptimal performance, especially when training data for downstream tasks is limited. The pre-pruning and sparse training methods can mitigate this issue to a certain extent, and building upon this, we further propose a hierar-

chical sparse strategy, as illustrated in Fig. 3. The adapter module consists of two parts: the down-projection layer and the up-projection layer. We keep the down-projection layer as a dense matrix, *i.e.*  $\mathcal{W}^{\text{down}} = \mathcal{W}^{\text{down}}$ , and only introduce sparsity in the up-projection layer, *i.e.*  $\mathcal{W}^{\text{up}} = \{\mathcal{W}_i^{\text{up}}\}_{i=1}^N$ . This adaptation process can be expressed as:

$$\tilde{x} \leftarrow x + f(x \cdot \mathcal{W}^{\text{down}}) \cdot \mathcal{W}_i^{\text{up}} \quad (5)$$

The dense down-projection layer provides robust intermediate features by receiving all training data, while multiple sparse up-projection layers map features to different subspaces, enhancing the performance on downstream tasks. Ablation experiments demonstrate the effectiveness of this hierarchical sparse strategy.

**Deep feature alignment.** Like [80] and [68], we also apply consistency regularization to ensure that different experts provide similar results for the same task. However, considering that different sparse adapters need to be merged after tuning, we further propose a deep feature alignment strategy to ensure that model parameters are not incompatible when merged. Given that deep features in neural networks are generally universal, while shallow features are typically task-specific, to strike a balance between model capacity and consistency, we align only the deep features of the model. Specifically, for a neural network with  $L$  layers, we align the features extracted by different experts in the first  $L/2$  layers. The overall optimization objective is formulated as follows:

$$\begin{aligned} \mathcal{L}(x, y) = & \text{CE}(p_1, y) + \frac{\alpha}{2} (\text{KL}(p_1 \| p_2) + \\ & \text{KL}(p_2 \| p_1)) + \beta \sum_{i=1}^{L/2} \text{MSE}(f_1^i, f_2^i) \end{aligned} \quad (6)$$

where  $p_1, p_2$  represent the predicted probabilities after two stochastic forward passes of  $x$ , and  $f_1^i, f_2^i$  represent the intermediate features in the  $i$ -th layer. Here, CE is the cross-entropy loss, KL is the Kullback–Leibler divergence and MSE is the mean square error.  $\alpha$  and  $\beta$  are hyper-parameters that control the weight of regularization terms.

### 3.4. Jigsaw-like adapter merging

During the inference stage, we merge the trained multiple sparse adapters like puzzle pieces into a complete adapter. The merging process can be expressed as follows:

$$\overline{\mathcal{W}}[\mathcal{M}_i > 0] \leftarrow \mathcal{W}_i[\mathcal{M}_i > 0] \quad (7)$$

Here,  $\mathcal{M}_i$  represents the sparse mask from Eq. (4). After the merge, the inference phase can be represented as:

$$\tilde{x} \leftarrow x + f(x \cdot \overline{\mathcal{W}^{\text{down}}}) \cdot \overline{\mathcal{W}^{\text{up}}} \quad (8)$$

Experiments demonstrate that the merged adapter outperforms stochastic activation during inference.

## 4. Experiments

### 4.1. Experimental setup

**Pre-trained backbones.** We experiment with two Transformer architectures in vision: ViT [13] and Swin Transformer [43]. In our experiments, all models are pre-trained on ImageNet-21k [60]. We adhere to the original configurations of these models, such as the number of image patches divided and the inclusion of the [CLS] token, etc. More details can be found in Appendix.

**Baselines.** We compare our MoSA with other Adapter Tuning methods and commonly used fine-tuning strategies:

- **Full fine-tuning:** fully update the whole backbone.
- **Linear probing:** fix the model backbone and update only a single-layer classifier.
- **BitFit (Bias)** [74]: fine-tune all the bias terms in the pre-trained backbone.
- **AdaptFormer** [6]: insert new bottleneck modules with residual connections inside Transformer blocks.
- **SparseAdapter** [24]: prune the standard adapter before tuning and update the remaining parameters.

**Downstream tasks.** We evaluate MoSA against other baselines on the following three collections of datasets:

- **FGVC:** This benchmark consists of 5 Fine-Grained Visual Classification tasks, including CUB-200-2011 [67], NABirds [65], Oxford Flowers [51], Stanford Dogs [12], and Stanford Cars [15], which are representative examples of this category. We directly adapt the public split for training and validation sets if available, or we just follow the splits in [29].
- **VTAB:** VTAB-1k [75] benchmark consists of 19 visual classification tasks from 3 diverse domains: *Natural*, *Specialized* and *Structured*. Each task contains only 1000 training examples, but potentially spanning up to 397 classes, poses a significant challenge.
- **GICD:** We also collect a benchmark of 3 General Image Classification Datasets, including CIFAR-100 [34], Aircraft [48] and Food-101 [4], to demonstrate the efficiency of MoSA. All the datasets comprise around 100 categories, each containing at least 10,000 images, all of which are common objects in natural scenes.

**Implementation details.** For all datasets, we only process the images with a randomly resized crop to  $224 \times 224$  and a random horizontal flip for data augmentation, instead of other strong augmentation and regularization strategies, like mixup [77] and cutmix [72]. We adopt the AdamW [45] optimizer to fine-tune the pre-trained model for 100 epochs, with a linear warm-up of the learning rate for the first 10 epochs. For a fair comparison, we set the general hyper-parameters to be the same in all Adaptor Tuning methods, including our MoSA. All experiments are conducted using the PyTorch [56] library on NVIDIA V100 and A100 GPUs. More implementation details can be found in Appendix.

Method \ Dataset	CUB-200 -2011	NABrids	Oxford Flowers	Stanford Dogs	Stanford Cars	Mean Acc. (%)	Mean Params. (M)
Full fine-tuning	87.3	82.7	98.8	89.4	<b>84.5</b>	88.54	85.80
Linear probing	85.3	75.9	97.9	86.2	51.3	79.32	0.00
BitFit [74]	<u>88.4</u>	84.2	98.8	91.2	79.4	88.40	0.10
AdaptFormer [6]	87.4	84.8	<u>99.0</u>	90.7	81.0	88.58	1.54
SparseAdapter [24]	87.8	<u>85.1</u>	98.9	<u>91.4</u>	80.3	<u>88.70</u>	0.39
MoSA (Ours)	<b>89.3</b>	<b>85.7</b>	<b>99.2</b>	<b>91.9</b>	<u>83.4</u>	<b>89.90</b>	1.54

Table 1. Results on FGVC with ViT-B/16 backbone pre-trained on ImageNet-21K.

Method \ Dataset	VTAB					GICD				
	Natural	Specialized	Structured	Mean Acc. (%)	Mean Params. (M)	CIFAR-100	Aircraft	Food-101	Mean Acc. (%)	Mean Params. (M)
Full fine-tuning	75.88	83.36	47.64	68.96	85.80	89.12	70.93	<u>90.96</u>	83.67	85.80
Linear probing	68.93	77.16	26.84	57.64	0.00	85.95	45.06	88.14	73.05	0.00
BitFit [74]	73.30	78.25	44.09	65.21	0.10	91.69	68.71	89.59	83.33	0.10
AdaptFormer [6]	<u>78.42</u>	<u>83.41</u>	<u>49.17</u>	<u>70.33</u>	0.30	<u>91.86</u>	<u>71.71</u>	90.89	<u>84.82</u>	1.19
SparseAdapter [24]	77.58	81.99	48.26	69.28	0.08	91.20	67.15	89.37	82.57	0.30
MoSA (Ours)	<b>79.86</b>	<b>84.03</b>	<b>50.28</b>	<b>71.39</b>	0.30	<b>92.22</b>	<b>72.14</b>	<b>91.17</b>	<b>85.18</b>	1.19

Table 2. Results on VTAB and GICD with ViT-B/16 backbone pre-trained on ImageNet-21K.

## 4.2. Main Results

We provide a comprehensive evaluation of the effectiveness of our MoSA by comparing it with other baselines across 3 sets of up to 27 different datasets. We also combine five FGVC datasets together to form a complex multi-task benchmark, validating the enhancement of model capacity through the mixed training of multiple sparse experts. More experiments on different model architectures, adapter structures and PEFT methods (*e.g.*, LoRA) can be found in Appendix. In the following experiments, Top-1 accuracy (%) is used to evaluate the performance of the methods on the respective datasets, and the number (M) of extra parameters (trainable parts excluding the classifier) is used to assess the efficiency of the methods. The best accuracy is highlighted in **bold**, while the second one is underlined.

**Fine-grained classification performance.** We first evaluate the effectiveness of our method in transfer learning on 5 fine-grained visual classification tasks with ViT-B/16 [13] backbone. As shown in Tab. 1, our MoSA beats other fine-tuning baselines, including full fine-tuning, by a significant margin. Across the 5 downstream tasks, MoSA achieves an average accuracy of 89.90%, surpassing full fine-tuning and AdaptFormer [6] by 1.36% and 1.32%, respectively, while maintaining the same number of trainable parameters as [6]. Interestingly, SparseAdapter [24], with fewer trainable parameters just through pruning, outperforms the standard adapter by 0.12% on average, demonstrating the parameter redundancy in adapters for visual

tasks. However, the high sparsity level results in ineffective utilization of most parameters in the adapter, limiting the overall performance gain. Our MoSA increases model capacity by mixed training of multiple sparse adapters, achieving an additional improvement of 1.20%. Experiments show that our method enhances the performance of existing methods without introducing extra parameters or computation, maximizing the potential of adapters.

**Low-resource visual adaptation performance.** We also compare our method with other fine-tuning approaches on VTAB, which contains 19 diverse downstream tasks with only 1000 training samples per task, making it extremely challenging. Previous stochastically activated MoE methods, like [80], suffer from severe performance degradation when training data is insufficient. However, our MoSA overcomes this issue with its hierarchical sparse strategy. The results in Tab. 2 demonstrate that MoSA outperforms all other baselines by updating only 0.35% (0.30M in 85.80M) of the pre-trained backbone parameters. Specifically, across 3 domains in VTAB, MoSA surpasses full fine-tuning by 3.98%, 0.67% and 2.64%, while outperforming the second-best AdaptFormer by 1.44%, 0.62% and 1.11%, providing strong evidence for the effectiveness of our hierarchical sparse design.

**General large-scale classification performance.** To further evaluate the generality of our method, we compare MoSA with other fine-tuning methods on 3 general classification tasks, as shown in Tab. 2. MoSA outperforms all baselines, including full fine-tuning, on all 3 datasets.

Method	FGVC-multi (%)	Params. (M)
Full fine-tuning	77.80	85.80
Linear probing	67.06	0.00
BitFit [74]	75.96	0.10
AdaptFormer [6]	78.28	2.42
SparseAdapter [24]	78.08	0.60
MoSA (Ours)	<b>78.59</b>	2.42

Table 3. Results on FGVC-multi with ViT-B/16 backbone pre-trained on ImageNet-21K.

Specifically, compared to AdaptFormer and full fine-tuning, MoSA achieves an average accuracy improvement of 1.51% and 0.36%, respectively, without introducing any additional parameters. It is worth noting that SparseAdapter performs poorly on this benchmark, exhibiting an accuracy drop of 2.25% compared to the standard adapter. This is attributed to the fact that the three datasets in GICD contain relatively sufficient training data, mitigating the advantages of sparsity. However, our method, through the combination of sparse training and MoE, demonstrates robust performance in scenarios with both abundant and limited training data, outperforming SparseAdapter by 2.61%, which proves the soundness of our design.

**Multi-task classification performance.** In contrast to typical classification tasks, we mix the 5 datasets in FGVC to form a more challenging multi-task classification scenario, showcasing the superiority of our approach. Tab. 3 shows the comparison results against other baselines, with MoSA outperforming full fine-tuning by 0.79%, demonstrating the outstanding performance of sparse MoE design in multi-task settings. AdaptFormer and SparseAdapter achieve 78.28% and 78.08% accuracy respectively, while MoSA beats them by 0.31% and 0.51%, indicating that standalone sparse training takes a toll on performance, whereas its combination with MoE leads to improvements.

### 4.3. Ablation Study

We conduct comprehensive ablation studies to verify the effectiveness of each component in our MoSA design. All ablation experiments are performed on FGVC with ViT-B backbone, and the performances of different strategies are measured using mean accuracy over the datasets.

**Hierarchical sparse strategy.** The MoE system increases the model capacity, while the sparse gating mechanism also leads to a decrease in the amount of data each expert encounters, resulting in suboptimal performance particularly when training data for downstream tasks is limited. In order to address this issue, we propose a hierarchical sparse strategy, and the results in Tab. 4 demonstrate the effectiveness of this design. Applying the sparse strategy to both

Strategy	Mean Acc. (%)
dense down + dense up	88.58
sparse down + sparse up	88.91
<b>dense down + sparse up</b>	<b>89.90</b>

Table 4. Effectiveness of hierarchical sparse strategy.

Regularization	Mean Acc. (%)
none	88.93
consistency	89.25
<b>consistency + alignment</b>	<b>89.90</b>

Table 5. Effectiveness of consistency regularization.

Mechanism	FLOPs	Mean Acc. (%)
fixed	$1\times$	88.42
stochastic	$1\times$	89.27
ensemble	$N\times$	88.63
<b>merge</b>	$1\times$	<b>89.90</b>

Table 6. Different mechanisms of inference.

the down-projection and up-projection layer only achieves an accuracy of 88.91%, slightly (0.33%) ahead of Adaptformer (dense down-projection and up-projection layer). However, with the hierarchical sparse strategy, we preserve the down-projection layer as a dense matrix while sparsely splitting the up-projection layer. In this way, MoSA outperforms Adaptformer by a large margin (89.90% vs. 88.58%), demonstrating the importance of this hierarchical strategy.

**Consistency regularization.** The mechanism of stochastic activation may lead to significant discrepancies among different experts, which can have adverse effects on the sparse module merging. In Tab. 5, we investigate the impact of regularization constraints in the training of MoSA. Without any regularization, our method achieves an accuracy of 88.93%. Applying consistency regularization on the final outputs of the model results in an improvement of 0.32%. And deep alignment of features extracted by different experts can further improve the accuracy by 0.65%.

**Merging vs. ensembling.** During inference, we merge multiple sparse adapters to form a complete adapter. However, [80] has pointed out that stochastic activation during inference can also achieve good performance. Therefore, we compare various inference methods, including fixed activation, stochastic activation, logits ensembling, and pa-

Expert number	1	2	3	4	5	8
Mean Acc. (%)	88.58	89.59	89.42	89.43	89.05	88.57

Table 7. Impact of expert number.

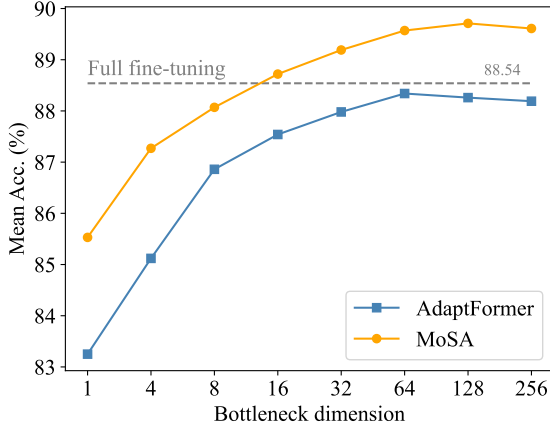


Figure 4. Impact of bottleneck dimensions of the adapter.

parameter merging. Results are presented in Tab. 6. It can be observed that fixed activation has the lowest accuracy, reaching only 88.41% on average. In comparison, stochastic activation achieves an improvement of 0.85%. Logits ensembling also leads to a certain improvement over fixed activation, but the increase of only 0.21% comes at the cost of  $N$  times the computational complexity ( $N$  refers to the number of experts), significantly reducing the inference speed. Finally, our parameter merging method achieves the best performance without any additional computation, further enhancing 0.63% over stochastic activation.

**Expert number.** To evaluate the compatibility between sparse training and MoE, we vary the number of splits in the adapters of MoSA during training, ranging from 1 to 5 and 8. The results are presented in Tab. 7. When the number of splits is set to 1, our method degrades to AdaptFormer. We can see that when the number of experts is between 2 and 5, indicating a sparsity level between 20% and 50% for the adapters, MoSA consistently achieves good performance. However, when the number of experts increases to 8, the performance experiences a noticeable decline due to excessive sparsity.

**Adapter bottleneck dimension.** Fig. 4 shows the impact of bottleneck dimensions of the adapter in AdaptFormer and MoSA. Overall, the performance shows an increasing trend followed by a decline as the number of trainable parameters increases. Across all bottleneck dimensions, MoSA consistently outperforms AdaptFormer, and our method can even surpass full fine-tuning with a bottleneck dimension of only 16. It is worth noting that the per-

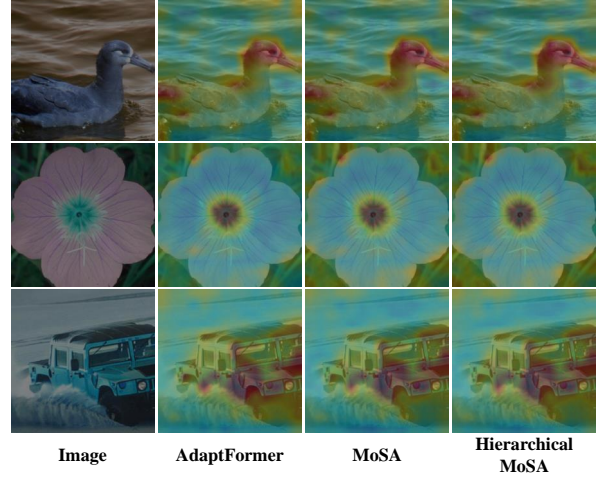


Figure 5. Attention map visualization.

formance of AdaptFormer starts to decline when the bottleneck dimension exceeds 64, while in our method, this turning point occurs at 128. This indicates that our design can more effectively utilize all parameters within the adapter.

#### 4.4. Visualization

Here, we use attention maps to visually illustrate the importance of the hierarchical sparse strategy. It can be observed that compared to AdaptFormer, our MoSA exhibits more focused attention on foreground objects (indicated by **darker** colors in Fig. 5), and the hierarchical sparse strategy further strengthens this attention. In the hierarchical sparse strategy, the dense down-projection layer provides robust intermediate features by receiving the entire training data, while multiple sparse up-projection layers project features into different subspaces for different data. The combination of the two components allows for better attention.

## 5. Conclusion

In this paper, we focus on the Adapter Tuning method in parameter-efficient fine-tuning and propose MoSA to improve the performance of standard adapters without any extra parameters or computation. Recognizing that standard adapters still suffer from parameter redundancy, we combine sparse training with stochastically activated MoE to fully utilize all parameters within the adapters. Comprehensive experiments on a total of 27 datasets show that MoSA consistently outperforms all other baselines, achieving state-of-the-art performance in Adapter Tuning. We hope that our work could inspire researchers to reconsider the issue of parameter redundancy in adapters and make further advancements towards more efficient PEFT methods.

## References

- [1] Alan Ansell, Edoardo Maria Ponti, Anna Korhonen, and Ivan Vulić. Composable sparse fine-tuning for cross-lingual transfer. *arXiv preprint arXiv:2110.07560*, 2021. 2, 3
- [2] Charles Beattie, Joel Z Leibo, Denis Teplyashin, Tom Ward, Marcus Wainwright, Heinrich Küttler, Andrew Lefrancq, Simon Green, Víctor Valdés, Amir Sadik, et al. Deepmind lab. *arXiv preprint arXiv:1612.03801*, 2016. 2
- [3] Yoshua Bengio. Deep learning of representations for unsupervised and transfer learning. In *Proceedings of ICML workshop on unsupervised and transfer learning*, pages 17–36. JMLR Workshop and Conference Proceedings, 2012. 1
- [4] Lukas Bossard, Matthieu Guillaumin, and Luc Van Gool. Food-101—mining discriminative components with random forests. In *Computer Vision—ECCV 2014: 13th European Conference, Zurich, Switzerland, September 6–12, 2014, Proceedings, Part VI 13*, pages 446–461. Springer, 2014. 5, 1, 2
- [5] Tom Brown, Benjamin Mann, Nick Ryder, Melanie Subbiah, Jared D Kaplan, Prafulla Dhariwal, Arvind Neelakantan, Pranav Shyam, Girish Sastry, Amanda Askell, et al. Language models are few-shot learners. *Advances in neural information processing systems*, 33:1877–1901, 2020. 2
- [6] Shoufa Chen, Chongjian Ge, Zhan Tong, Jiangliu Wang, Yibing Song, Jue Wang, and Ping Luo. Adaptformer: Adapting vision transformers for scalable visual recognition. *Advances in Neural Information Processing Systems*, 35:16664–16678, 2022. 2, 3, 5, 6, 7, 4
- [7] Ting Chen, Simon Kornblith, Mohammad Norouzi, and Geoffrey Hinton. A simple framework for contrastive learning of visual representations. In *International conference on machine learning*, pages 1597–1607. PMLR, 2020. 1
- [8] Tianrun Chen, Lanyun Zhu, Chaotao Ding, Runlong Cao, Shangzhan Zhang, Yan Wang, Zejian Li, Lingyun Sun, Papa Mao, and Ying Zang. Sam fails to segment anything?—sam-adapter: Adapting sam in underperformed scenes: Camouflage, shadow, and more. *arXiv preprint arXiv:2304.09148*, 2023. 2
- [9] X Chen, S Xie, and K He. An empirical study of training self-supervised vision transformers. In *CVF International Conference on Computer Vision (ICCV)*, pages 9620–9629, 2021. 1
- [10] Gong Cheng, Junwei Han, and Xiaoqiang Lu. Remote sensing image scene classification: Benchmark and state of the art. *Proceedings of the IEEE*, 105(10):1865–1883, 2017. 2
- [11] Mircea Cimpoi, Subhansu Maji, Iasonas Kokkinos, Sammy Mohamed, and Andrea Vedaldi. Describing textures in the wild. In *Proceedings of the IEEE conference on computer vision and pattern recognition*, pages 3606–3613, 2014. 2
- [12] E Dataset. Novel datasets for fine-grained image categorization. In *First Workshop on Fine Grained Visual Categorization, CVPR. Citeseer. Citeseer*. Citeseer, 2011. 5, 1, 2
- [13] Alexey Dosovitskiy, Lucas Beyer, Alexander Kolesnikov, Dirk Weissenborn, Xiaohua Zhai, Thomas Unterthiner, Mostafa Dehghani, Matthias Minderer, Georg Heigold, Sylvain Gelly, et al. An image is worth 16x16 words: Transformers for image recognition at scale. *arXiv preprint arXiv:2010.11929*, 2020. 2, 3, 5, 6
- [14] Li Fei-Fei, Robert Fergus, and Pietro Perona. One-shot learning of object categories. *IEEE transactions on pattern analysis and machine intelligence*, 28(4):594–611, 2006. 2
- [15] Timnit Gebru, Jonathan Krause, Yilun Wang, Duyun Chen, Jia Deng, and Li Fei-Fei. Fine-grained car detection for visual census estimation. In *Proceedings of the AAAI Conference on Artificial Intelligence*, 2017. 5, 1, 2
- [16] Andreas Geiger, Philip Lenz, Christoph Stiller, and Raquel Urtasun. Vision meets robotics: The kitti dataset. *The International Journal of Robotics Research*, 32(11):1231–1237, 2013. 2
- [17] Priya Goyal, Piotr Dollár, Ross Girshick, Pieter Noordhuis, Lukasz Wesolowski, Aapo Kyrola, Andrew Tulloch, Yangqing Jia, and Kaiming He. Accurate, large mini-batch sgd: Training imagenet in 1 hour. *arXiv preprint arXiv:1706.02677*, 2017. 1
- [18] Ben Graham. Kaggle diabetic retinopathy detection competition report. *University of Warwick*, pages 24–26, 2015. 2
- [19] Demi Guo, Alexander M Rush, and Yoon Kim. Parameter-efficient transfer learning with diff pruning. *arXiv preprint arXiv:2012.07463*, 2020. 2, 3
- [20] Song Han, Xingyu Liu, Huizi Mao, Jing Pu, Ardavan Pedram, Mark A Horowitz, and William J Dally. Eie: Efficient inference engine on compressed deep neural network. *ACM SIGARCH Computer Architecture News*, 44(3):243–254, 2016. 3
- [21] Haoyu He, Jianfei Cai, Jing Zhang, Dacheng Tao, and Bohan Zhuang. Sensitivity-aware visual parameter-efficient fine-tuning. In *Proceedings of the IEEE/CVF International Conference on Computer Vision*, pages 11825–11835, 2023. 3
- [22] Kaiming He, Haoqi Fan, Yuxin Wu, Saining Xie, and Ross Girshick. Momentum contrast for unsupervised visual representation learning. In *Proceedings of the IEEE/CVF conference on computer vision and pattern recognition*, pages 9729–9738, 2020. 1
- [23] Kaiming He, Xinlei Chen, Saining Xie, Yanghao Li, Piotr Dollár, and Ross Girshick. Masked autoencoders are scalable vision learners. In *Proceedings of the IEEE/CVF conference on computer vision and pattern recognition*, pages 16000–16009, 2022. 1, 2
- [24] Shwai He, Liang Ding, Daize Dong, Miao Zhang, and Dacheng Tao. Sparseadapter: An easy approach for improving the parameter-efficiency of adapters. *arXiv preprint arXiv:2210.04284*, 2022. 2, 3, 4, 5, 6, 7
- [25] Patrick Helber, Benjamin Bischke, Andreas Dengel, and Damian Borth. Eurosat: A novel dataset and deep learning benchmark for land use and land cover classification. *IEEE Journal of Selected Topics in Applied Earth Observations and Remote Sensing*, 12(7):2217–2226, 2019. 2
- [26] Neil Houlsby, Andrei Giurgiu, Stanislaw Jastrzebski, Bruna Morrone, Quentin De Laroussilhe, Andrea Gesmundo, Mona Attariyan, and Sylvain Gelly. Parameter-efficient transfer learning for nlp. In *International Conference on Machine Learning*, pages 2790–2799. PMLR, 2019. 2, 3, 1, 4
- [27] Edward J Hu, Yelong Shen, Phillip Wallis, Zeyuan Allen-Zhu, Yuanzhi Li, Shean Wang, Lu Wang, and Weizhu Chen.

- Lora: Low-rank adaptation of large language models. *arXiv preprint arXiv:2106.09685*, 2021. 2, 3, 4
- [28] Robert A Jacobs, Michael I Jordan, Steven J Nowlan, and Geoffrey E Hinton. Adaptive mixtures of local experts. *Neural computation*, 3(1):79–87, 1991. 3
- [29] Menglin Jia, Luming Tang, Bor-Chun Chen, Claire Cardie, Serge Belongie, Bharath Hariharan, and Ser-Nam Lim. Visual prompt tuning. In *European Conference on Computer Vision*, pages 709–727. Springer, 2022. 2, 3, 5, 1
- [30] Shibo Jie and Zhi-Hong Deng. Fact: Factor-tuning for lightweight adaptation on vision transformer. In *Proceedings of the AAAI Conference on Artificial Intelligence*, pages 1060–1068, 2023. 3
- [31] Justin Johnson, Bharath Hariharan, Laurens Van Der Maaten, Li Fei-Fei, C Lawrence Zitnick, and Ross Girshick. Clevr: A diagnostic dataset for compositional language and elementary visual reasoning. In *Proceedings of the IEEE conference on computer vision and pattern recognition*, pages 2901–2910, 2017. 2
- [32] Alexander Kirillov, Eric Mintun, Nikhila Ravi, Hanzi Mao, Chloe Rolland, Laura Gustafson, Tete Xiao, Spencer Whitehead, Alexander C Berg, Wan-Yen Lo, et al. Segment anything. *arXiv preprint arXiv:2304.02643*, 2023. 1
- [33] Simon Kornblith, Jonathon Shlens, and Quoc V Le. Do better imagenet models transfer better? In *Proceedings of the IEEE/CVF conference on computer vision and pattern recognition*, pages 2661–2671, 2019. 1
- [34] Alex Krizhevsky. Learning multiple layers of features from tiny images. *University of Toronto*, 2012. 5, 1, 2
- [35] Alex Krizhevsky. One weird trick for parallelizing convolutional neural networks. *arXiv preprint arXiv:1404.5997*, 2014. 1
- [36] Yann LeCun, Fu Jie Huang, and Leon Bottou. Learning methods for generic object recognition with invariance to pose and lighting. In *Proceedings of the 2004 IEEE Computer Society Conference on Computer Vision and Pattern Recognition, 2004. CVPR 2004.*, pages II–104. IEEE, 2004. 2
- [37] Brian Lester, Rami Al-Rfou, and Noah Constant. The power of scale for parameter-efficient prompt tuning. *arXiv preprint arXiv:2104.08691*, 2021. 2, 3
- [38] Xiang Lisa Li and Percy Liang. Prefix-tuning: Optimizing continuous prompts for generation. *arXiv preprint arXiv:2101.00190*, 2021.
- [39] Dongze Lian, Daquan Zhou, Jiashi Feng, and Xinchao Wang. Scaling & shifting your features: A new baseline for efficient model tuning. *Advances in Neural Information Processing Systems*, 35:109–123, 2022. 2
- [40] Haokun Liu, Derek Tam, Mohammed Muqeeth, Jay Mohta, Tenghao Huang, Mohit Bansal, and Colin A Raffel. Few-shot parameter-efficient fine-tuning is better and cheaper than in-context learning. *Advances in Neural Information Processing Systems*, 35:1950–1965, 2022. 3
- [41] Xiao Liu, Kaixuan Ji, Yicheng Fu, Weng Tam, Zhengxiao Du, Zhilin Yang, and Jie Tang. P-tuning: Prompt tuning can be comparable to fine-tuning across scales and tasks. In *Proceedings of the 60th Annual Meeting of the Association for Computational Linguistics (Volume 2: Short Papers)*, pages 61–68, 2022. 2
- [42] Yuanhan Zhang Kaiyang Zhou Ziwei Liu. Neural prompt search. *arXiv preprint arXiv:2206.04673*, 2022. 3
- [43] Ze Liu, Yutong Lin, Yue Cao, Han Hu, Yixuan Wei, Zheng Zhang, Stephen Lin, and Baining Guo. Swin transformer: Hierarchical vision transformer using shifted windows. In *Proceedings of the IEEE/CVF international conference on computer vision*, pages 10012–10022, 2021. 5, 1
- [44] Ilya Loshchilov and Frank Hutter. Sgdr: Stochastic gradient descent with warm restarts. *arXiv preprint arXiv:1608.03983*, 2016. 2
- [45] Ilya Loshchilov and Frank Hutter. Decoupled weight decay regularization. *arXiv preprint arXiv:1711.05101*, 2017. 5, 2
- [46] He Lyu, Ningyu Sha, Shuyang Qin, Ming Yan, Yuying Xie, and Rongrong Wang. Advances in neural information processing systems. *Advances in neural information processing systems*, 32, 2019. 3
- [47] Jiaqi Ma, Zhe Zhao, Xinyang Yi, Jilin Chen, Lichan Hong, and Ed H Chi. Modeling task relationships in multi-task learning with multi-gate mixture-of-experts. In *Proceedings of the 24th ACM SIGKDD international conference on knowledge discovery & data mining*, pages 1930–1939, 2018. 3
- [48] Subhransu Maji, Esa Rahtu, Juho Kannala, Matthew Blaschko, and Andrea Vedaldi. Fine-grained visual classification of aircraft. *arXiv preprint arXiv:1306.5151*, 2013. 5, 1, 2
- [49] Loic Matthey, Irina Higgins, Demis Hassabis, and Alexander Lerchner. dsprites: Disentanglement testing sprites dataset, 2017. 2
- [50] Dmitry Molchanov, Arsenii Ashukha, and Dmitry Vetrov. Variational dropout sparsifies deep neural networks. In *International Conference on Machine Learning*, pages 2498–2507. PMLR, 2017. 3
- [51] Maria-Elena Nilsback and Andrew Zisserman. Automated flower classification over a large number of classes. In *2008 Sixth Indian conference on computer vision, graphics & image processing*, pages 722–729. IEEE, 2008. 5, 1, 2
- [52] Junting Pan, Ziyi Lin, Xiatian Zhu, Jing Shao, and Hongsheng Li. St-adapter: Parameter-efficient image-to-video transfer learning. *Advances in Neural Information Processing Systems*, 35:26462–26477, 2022. 2, 3
- [53] Sinno Jialin Pan and Qiang Yang. A survey on transfer learning. *IEEE Transactions on knowledge and data engineering*, 22(10):1345–1359, 2009. 1
- [54] Jungin Park, Jiyoung Lee, and Kwanghoon Sohn. Dual-path adaptation from image to video transformers. In *Proceedings of the IEEE/CVF Conference on Computer Vision and Pattern Recognition*, pages 2203–2213, 2023. 2, 3
- [55] Omkar M Parkhi, Andrea Vedaldi, Andrew Zisserman, and CV Jawahar. Cats and dogs. In *2012 IEEE conference on computer vision and pattern recognition*, pages 3498–3505. IEEE, 2012. 2
- [56] Adam Paszke, Sam Gross, Francisco Massa, Adam Lerer, James Bradbury, Gregory Chanan, Trevor Killeen, Zeming

- Lin, Natalia Gimelshein, Luca Antiga, et al. Pytorch: An imperative style, high-performance deep learning library. *Advances in neural information processing systems*, 32, 2019. 5
- [57] Jonas Pfeiffer, Aishwarya Kamath, Andreas Rücklé, Kyunghyun Cho, and Iryna Gurevych. Adapterfusion: Non-destructive task composition for transfer learning. *arXiv preprint arXiv:2005.00247*, 2020. 2, 3, 1, 4
- [58] Jonas Pfeiffer, Andreas Rücklé, Clifton Poth, Aishwarya Kamath, Ivan Vulić, Sebastian Ruder, Kyunghyun Cho, and Iryna Gurevych. Adapterhub: A framework for adapting transformers. *arXiv preprint arXiv:2007.07779*, 2020. 2
- [59] Carlos Riquelme, Joan Puigcerver, Basil Mustafa, Maxim Neumann, Rodolphe Jenatton, André Susano Pinto, Daniel Keysers, and Neil Houlsby. Scaling vision with sparse mixture of experts. *Advances in Neural Information Processing Systems*, 34:8583–8595, 2021. 2
- [60] Olga Russakovsky, Jia Deng, Hao Su, Jonathan Krause, Sanjeev Satheesh, Sean Ma, Zhiheng Huang, Andrej Karpathy, Aditya Khosla, Michael Bernstein, et al. Imagenet large scale visual recognition challenge. *International journal of computer vision*, 115:211–252, 2015. 1, 5
- [61] Noam Shazeer, Azalia Mirhoseini, Krzysztof Maziarczyk, Andy Davis, Quoc Le, Geoffrey Hinton, and Jeff Dean. Outrageously large neural networks: The sparsely-gated mixture-of-experts layer. *arXiv preprint arXiv:1701.06538*, 2017. 2, 3, 4
- [62] Chen Sun, Abhinav Shrivastava, Saurabh Singh, and Abhinav Gupta. Revisiting unreasonable effectiveness of data in deep learning era. In *Proceedings of the IEEE international conference on computer vision*, pages 843–852, 2017. 1
- [63] Hugo Touvron, Louis Martin, Kevin Stone, Peter Albert, Amjad Almahairi, Yasmine Babaei, Nikolay Bashlykov, Soumya Batra, Prajwal Bhargava, Shruti Bhosale, et al. Llama 2: Open foundation and fine-tuned chat models. *arXiv preprint arXiv:2307.09288*, 2023. 2
- [64] Laurens Van der Maaten and Geoffrey Hinton. Visualizing data using t-sne. *Journal of machine learning research*, 9 (11), 2008. 3
- [65] Grant Van Horn, Steve Branson, Ryan Farrell, Scott Haber, Jessie Barry, Panos Ipeirotis, Pietro Perona, and Serge Belongie. Building a bird recognition app and large scale dataset with citizen scientists: The fine print in fine-grained dataset collection. In *Proceedings of the IEEE conference on computer vision and pattern recognition*, pages 595–604, 2015. 5, 1, 2
- [66] Bastiaan S Veeling, Jasper Linmans, Jim Winkens, Taco Cohen, and Max Welling. Rotation equivariant cnns for digital pathology. In *Medical Image Computing and Computer Assisted Intervention—MICCAI 2018: 21st International Conference, Granada, Spain, September 16-20, 2018, Proceedings, Part II*, pages 210–218. Springer, 2018. 2
- [67] Catherine Wah, Steve Branson, Peter Welinder, Pietro Perona, and Serge Belongie. The caltech-ucsd birds-200-2011 dataset. Technical Report CNS-TR-2011-001, California Institute of Technology, 2011. 5, 1, 2
- [68] Yaqing Wang, Sahaj Agarwal, Subhabrata Mukherjee, Xiaodong Liu, Jing Gao, Ahmed Hassan Awadallah, and Jianfeng Gao. Adamix: Mixture-of-adaptations for parameter-efficient model tuning. *arXiv preprint arXiv:2210.17451*, 2022. 4, 5
- [69] Jianxiong Xiao, James Hays, Krista A Ehinger, Aude Oliva, and Antonio Torralba. Sun database: Large-scale scene recognition from abbey to zoo. In *2010 IEEE computer society conference on computer vision and pattern recognition*, pages 3485–3492. IEEE, 2010. 2
- [70] Runxin Xu, Fuli Luo, Zhiyuan Zhang, Chuanqi Tan, Baobao Chang, Songfang Huang, and Fei Huang. Raise a child in large language model: Towards effective and generalizable fine-tuning. *arXiv preprint arXiv:2109.05687*, 2021. 2, 3
- [71] Jason Yosinski, Jeff Clune, Yoshua Bengio, and Hod Lipson. How transferable are features in deep neural networks? *Advances in neural information processing systems*, 27, 2014. 1
- [72] Sangdoo Yun, Dongyoon Han, Seong Joon Oh, Sanghyuk Chun, Junsuk Choe, and Youngjoon Yoo. Cutmix: Regularization strategy to train strong classifiers with localizable features. In *Proceedings of the IEEE/CVF international conference on computer vision*, pages 6023–6032, 2019. 5
- [73] Netzer Yuval. Reading digits in natural images with unsupervised feature learning. In *Proceedings of the NIPS Workshop on Deep Learning and Unsupervised Feature Learning*, 2011. 2
- [74] Elad Ben Zaken, Shauli Ravfogel, and Yoav Goldberg. Bitfit: Simple parameter-efficient fine-tuning for transformer-based masked language-models. *arXiv preprint arXiv:2106.10199*, 2021. 2, 3, 5, 6, 7, 4
- [75] Xiaohua Zhai, Joan Puigcerver, Alexander Kolesnikov, Pierre Ruysen, Carlos Riquelme, Mario Lucic, Josip Djolonga, Andre Susano Pinto, Maxim Neumann, Alexey Dosovitskiy, et al. A large-scale study of representation learning with the visual task adaptation benchmark. *arXiv preprint arXiv:1910.04867*, 2019. 5, 1, 2
- [76] Xiaohua Zhai, Alexander Kolesnikov, Neil Houlsby, and Lucas Beyer. Scaling vision transformers. In *Proceedings of the IEEE/CVF Conference on Computer Vision and Pattern Recognition*, pages 12104–12113, 2022. 1
- [77] Hongyi Zhang, Moustapha Cisse, Yann N Dauphin, and David Lopez-Paz. mixup: Beyond empirical risk minimization. *arXiv preprint arXiv:1710.09412*, 2017. 5
- [78] Zhengyan Zhang, Yankai Lin, Zhiyuan Liu, Peng Li, Maosong Sun, and Jie Zhou. Moefication: Transformer feed-forward layers are mixtures of experts. *arXiv preprint arXiv:2110.01786*, 2021. 2, 3, 4
- [79] Fuzhen Zhuang, Zhiyuan Qi, Keyu Duan, Dongbo Xi, Yongchun Zhu, Hengshu Zhu, Hui Xiong, and Qing He. A comprehensive survey on transfer learning. *Proceedings of the IEEE*, 109(1):43–76, 2020. 1
- [80] Simiao Zuo, Xiaodong Liu, Jian Jiao, Young Jin Kim, Hany Hassan, Ruofei Zhang, Tuo Zhao, and Jianfeng Gao. Taming sparsely activated transformer with stochastic experts. *arXiv preprint arXiv:2110.04260*, 2021. 3, 4, 5, 6, 7

# Split & Merge: Unlocking the Potential of Visual Adapters via Sparse Training

## Supplementary Material

In this supplementary material, we present detailed information about the datasets and implementation of the experiments, along with additional experimental results of MoSA across different structures and additional visualizations. In Sec. A, we show details about all the datasets used in experiments. In Sec. B, we provide details about the experimental configurations. In Sec. C, we conduct additional experiments of MoSA on different backbone scales, model architectures, adapter structures, and PEFT methods. In Sec. D, we give additional visualization results.

### A. Dataset details

Here, we describe the details of all datasets used to validate MoSA. The number of classes and the train/valid/test splits for each dataset are shown in Tab. 8.

- **FGVC**: Fine-Grained Visual Classification (FGVC) benchmark consists of 5 downstream tasks, which are CUB-200-2011 [67], NABirds [65], Oxford Flowers [51], Stanford Dogs [12] and Stanford Cars [15]. Each task contains more than 100 classes and a few thousand images.
- **VTAB**: Visual Task Adaptation Benchmark [75] (VTAB) contains 19 visual classification tasks grouped into 3 domains: (1) *Natural* - tasks with natural images captured by standard cameras; (2) *Specialized* - tasks with images captured via specialized equipment, e.g. medical camera and satellite sensor; (3) *Structured* - tasks with images synthesized from simulated environments, which require geometric comprehension like object counting and depth estimation. Each task of VTAB contains only 1000 training samples, but may span up to 397 classes with several thousand testing samples, making it highly challenging.
- **GICD**: General Image Classification Datasets (GICD) benchmark consists of 3 general classification tasks, which are CIFAR-100 [34], Aircraft [48] and Food-101 [4]. All the tasks comprise around 100 classes, each containing at least 10,000 images, all of which are common objects in natural scenes.

### B. Implementation details

In Tab. 9, we summarize all experimental configurations with Adapter Tuning and LoRA. For other baselines, we just follow the settings in [29]. Following the linear scaling rule [9, 17, 23, 35], the learning rate is set as  $base\_lr \times b/256$ , where  $b$  is the batch size and  $base\_lr$  is chosen from the range specified in Tab. 9.

### C. More experiments

In this section, we validate the performance of MoSA on different backbone scales, model architectures, adapter structures, and PEFT methods. We also show the pre-task results for MoSA with ViT-B/16 on VTAB-1k. Similar to the main text, Top-1 accuracy (%) is used to evaluate the performance of the methods on the respective datasets, and the number (M) of extra parameters (trainable parts excluding the classifier) is used to assess the efficiency of the methods. The best accuracy is highlighted in **bold**, while the second one is underlined.

**MoSA on different backbone scales.** Here we evaluate MoSA with a larger backbone ViT-L/16 (303.3M vs. 85.8M ViT-B/16). The results in Tab. 10 indicate that, with the increase in backbone scale, the performance of the standard adapter cannot surpass full fine-tuning (89.70% vs. 90.16%). Sparse training could improve the performance of adapters, leading by 0.58% and 0.12% over the standard adapter and full fine-tuning, respectively. Our MoSA further enhances the performance by 0.78%, outperforming full fine-tuning by a large margin.

**MoSA on different model architectures.** In addition to the standard ViT, we also experiment with another hierarchical vision Transformer, Swin-B [43], to demonstrate the effectiveness of MoSA. Similar to ViT, we can easily apply MoSA to Swin. As shown in Tab. 11, due to the strong feature extraction capability of this model architecture, full fine-tuning performs well on Swin, while other PEFT methods show suboptimal performance. It’s worth noting that our MoSA is the only method that outperforms full fine-tuning on Swin (90.72% vs. 90.14%), indicating that MoSA consistently adapts various vision Transformers to downstream tasks and improves performance.

**MoSA on different adapter structures.** As a supplement, we apply MoSA to two different adapter structures: Pfeiffer [57] and Houlsby [26]. Both Pfeiffer and Houlsby use a sequential connection for adapter design, with Pfeiffer incorporating the adapters only after the FFN layers, while Houlsby includes the adapters after both the Attention and FFN layers. The performance comparison on the two adapter structures is shown in Tab. 12. In this experiment, the bottleneck dimension for all adapters is set to 64. It can be observed that on both structures, sparse training brings improvements of 1.50% and 1.30% over the standard adapter, and the corresponding versions of our MoSA further yield performance gains of 1.70% and 1.76%.

Dataset		#Classes	Train	Val	Test
Fine-Grained Visual Classification (FGVC)					
CUB-200-2011 [67]		200	5,394	600	5,794
NABirds [65]		555	21,536	2,393	24,633
Oxford Flowers [51]		102	1,020	1,020	6,149
Stanford Dogs [12]		120	10,800	1,200	8,580
Stanford Cars [15]		196	7,329	815	8,041
Visual Task Adaptation Benchmark (VTAB) [75]					
Natural	CIFAR-100 [34]	100			10,000
	Caltech101 [14]	102			6,084
	DTD [11]	47			1,880
	Flowers102 [51]	102	800/1000	200	6,149
	Pets [55]	37			3,669
	SVHN [73]	10			26,032
	Sun397 [69]	397			21,750
Specialized	Patch Camelyon [66]	2			32,768
	EuroSAT [25]	10			5,400
	Resisc45 [10]	45	800/1000	200	6,300
	Retinopathy [18]	5			42,670
Structured	Clevr/count [31]	8			15,000
	Clevr/distance [31]	6			15,000
	DMLab [2]	6			22,735
	KITTI/distance [16]	4			711
	dSprites/location [49]	16	800/1000	200	73,728
	dSprites/orientation [49]	16			73,728
	SmallNORB/azimuth [36]	18			12,150
	SmallNORB/elevation [36]	9			12,150
General Image Classification Datasets (GICD)					
CIFAR-100 [34]		100	50,000	-	10,000
Aircraft [48]		100	3,334	3,333	3,333
Food-101 [4]		101	75,750	-	25,250

Table 8. Details of all datasets used to validate MoSA.

Configuration	Value
Optimizer	AdamW [45]
Base learning rate range	{0.01, 0.005, 0.001, 0.0005, 0.0001}
Weight decay range	{0.01, 0.0}
Learning rate schedule	cosine decay [44]
Batch size	128 (ViT-B/16, Swin-B), 64 (ViT-L/16)
Warmup epoch	10
Total epoch	100 (ViT-B/16, Swin-B), 50 (ViT-L/16)
Augmentation	RandomResizedCrop [23], RandomHorizontalFlip

Table 9. Implementation details for Adapter Tuning and LoRA.

**MoSA on different PEFT methods.** To demonstrate the generality of our approach, we choose another widely

used PEFT method, namely LoRA [27]. LoRA achieves parameter-efficient fine-tuning by applying a low-rank de-

Method \ Dataset	CUB-200 -2011	NABrids	Oxford Flowers	Stanford Dogs	Stanford Cars	Mean Acc. (%)	Mean Params. (M)
Full fine-tuning	88.3	85.9	96.7	93.1	<b>86.8</b>	90.16	303.30
Linear probing	84.7	78.9	97.4	89.6	55.1	81.14	0.00
BitFit [74]	88.5	86.4	98.8	93.5	83.2	90.08	0.27
AdaptFormer-64 [6]	89.3	86.3	98.8	93.2	80.9	89.70	3.17
SparseAdapter-64 [24]	<u>89.4</u>	<u>86.8</u>	<u>99.0</u>	<u>93.9</u>	82.3	<u>90.28</u>	0.79
MoSA-64 (Ours)	<b>89.7</b>	<b>87.2</b>	<b>99.4</b>	<b>94.5</b>	<u>84.9</u>	<b>91.06</b>	3.17

Table 10. Results on FGVC with ViT-L/16 backbone pre-trained on ImageNet-21K.

Method \ Dataset	CUB-200 -2011	NABrids	Oxford Flowers	Stanford Dogs	Stanford Cars	Mean Acc. (%)	Mean Params. (M)
Full fine-tuning	88.2	<b>87.8</b>	99.0	85.5	<b>90.2</b>	<u>90.14</u>	86.74
Linear probing	87.8	83.8	98.8	84.7	69.2	84.86	0.00
BitFit [74]	88.4	85.2	99.2	85.3	83.4	88.30	0.20
AdaptFormer-64 [6]	<u>89.7</u>	<u>87.7</u>	99.3	86.0	<u>87.7</u>	90.08	1.55
SparseAdapter-64 [24]	<u>89.7</u>	87.4	<u>99.4</u>	<u>87.1</u>	86.8	90.08	0.39
MoSA-64 (Ours)	<b>90.6</b>	<b>87.8</b>	<b>99.6</b>	<b>88.3</b>	87.3	<b>90.72</b>	1.55

Table 11. Results on FGVC with Swin-B backbone pre-trained on ImageNet-21K.

composition to the weight updates of linear layers. During inference, the additional modules could be merged into the pre-trained model parameters, resulting in zero extra overhead during inference. In Tab. 13, we compare the LoRA version sparse adapter (namely SparseLoRA) and our MoSA (namely MoSL) with the standard LoRA, with the rank of all LoRA modules set to 16. Our MoSL outperforms both the standard and sparse versions of LoRA, achieving an improvement of 1.48%, further confirming the effectiveness and rationality of our design.

**Per-task results for MoSA on VTAB-1k.** Tab. 14 shows the per-task results of MoSA on VTAB-1k. It can be seen that MoSA outperforms full fine-tuning on 13 tasks of VTAB, the highest among all PEFT methods. Additionally, MoSA also surpasses full fine-tuning (68.25% vs. 65.57%) and other baselines (AdaptFormer 67.16%) in the average accuracy across 19 tasks.

## D. More visualizations

**Attention map.** Here, we present more attention map visualizations in Fig. 6. Compared to AdaptFormer, our MoSA focuses more on foreground objects and exhibits more concentrated attention (highlighted in **red** in the images). And the hierarchical sparse strategy further strengthens this attention, providing intuitive evidence of the effectiveness of our design.

**t-SNE [64].** We also provide t-SNE visualizations to show the feature distribution of different methods on the CIFAR-100 dataset. The results are shown in Fig. 7. We can observe that our MoSA achieves better feature clustering compared to full fine-tuning and other PEFT baselines.

## E. Pipeline

### Algorithm 1 Pipeline of MoSA

---

**Require:** adapter paramters  $w$ , expert number  $N$   
 $\{w_i\}_{i=1}^N \leftarrow \text{Split}(w)$ ;  
**for** each epoch **do**  
  **for** each training batch  $x$  **do**  
     $w_j \leftarrow \text{StochasticActive}(\{w_i\}_{i=1}^N)$ ;  
    ForwardOneBatch( $w_j, x$ );  
  **end for**  
   $w^* \leftarrow \text{Merge}(\{w_i\}_{i=1}^N)$ ;  
  Evaluate( $w^*, x^{\text{test}}, y^{\text{test}}$ );  
**end for**

---

We demonstrate the pipeline of our MoSA with pseudo-code in Algorithm 1.

Method \ Dataset	CUB-200 -2011	NABrids	Oxford Flowers	Stanford Dogs	Stanford Cars	Mean Acc. (%)	Mean Params. (M)
Adapter-Pfeiffer [57]	84.5	81.3	97.9	88.8	76.7	85.84	1.21
SparseAdapter-Pfeiffer [24]	86.7	83.9	98.5	90.0	77.6	87.34	0.30
MoSA-Pfeiffer (Ours)	<b>89.3</b>	<b>85.5</b>	<b>99.2</b>	<b>91.6</b>	<b>79.6</b>	<b>89.04</b>	1.21
Adapter-Houlsby [26]	87.5	81.9	97.9	89.0	75.7	86.40	2.38
SparseAdapter-Houlsby [24]	87.5	83.3	98.9	90.1	78.7	87.70	0.59
MoSA-Houlsby (Ours)	<b>89.3</b>	<b>86.2</b>	<b>99.3</b>	<b>92.1</b>	<b>80.4</b>	<b>89.46</b>	2.38

Table 12. Results on FGVC with different adapter structures.

Method \ Dataset	CUB-200 -2011	NABrids	Oxford Flowers	Stanford Dogs	Stanford Cars	Mean Acc. (%)	Mean Params. (M)
LoRA-16 [27]	87.2	83.5	98.6	89.3	83.7	88.44	0.59
SparseLoRA-16 [24]	87.4	84.9	98.9	91.1	79.9	88.44	0.15
MoSL-16 (Ours)	<b>89.0</b>	<b>85.6</b>	<b>99.3</b>	<b>91.8</b>	<b>83.9</b>	<b>89.92</b>	0.59

Table 13. Results on FGVC with LoRA.

Method \ Dataset	Natural								Specialized				Structured				VTAB				
	CIFAR-100	Caltech101	DTD	Flowers102	Pets	SVHN	Sun397	Patch Camelyon	EuroSAT	Resisc45	Retinopathy	Clevr/count	Clevr/distance	DMLab	KITTI/distance	dSprites/loc	dSprites/ori	SmallINORB/azi	SmallINORB/ele	Mean Acc. (%)	Mean Params. (M)
Full fine-tuning	68.9	87.7	64.3	97.2	86.9	<b>87.4</b>	38.8	79.7	<b>95.7</b>	<b>84.2</b>	73.9	56.3	<b>58.6</b>	<b>41.7</b>	65.5	<u>57.5</u>	<b>46.7</b>	<u>25.7</u>	29.1	65.57	85.80
Linear probing	63.4	85.0	64.3	97.0	86.3	36.6	51.0	78.5	87.5	68.6	74.0	34.3	30.6	33.2	55.4	12.5	20.0	9.6	19.2	53.00	0.00
BitFit [74]	72.8	87.0	59.2	97.5	85.3	59.9	51.4	78.7	91.6	72.9	69.8	61.5	55.6	32.4	55.9	66.6	40.0	15.7	25.1	62.05	0.10
AdaptFormer [6]	78.9	<u>90.0</u>	<b>67.0</b>	<u>98.7</u>	89.0	72.2	<u>53.2</u>	<u>81.5</u>	<b>95.7</b>	81.2	<b>75.2</b>	70.6	57.4	39.3	<u>70.6</u>	54.5	42.4	25.3	<u>33.3</u>	<u>67.16</u>	0.30
SparseAdapter [24]	<u>79.1</u>	89.2	65.7	98.6	<u>89.3</u>	68.5	52.5	79.5	94.7	79.4	74.4	70.2	56.9	37.8	<b>70.9</b>	51.3	41.3	25.2	32.5	66.16	0.08
MoSA (Ours)	<b>79.7</b>	<b>91.5</b>	<u>66.2</u>	<b>98.8</b>	<b>89.7</b>	<u>79.0</u>	<b>53.4</b>	<b>83.4</b>	<u>95.6</u>	<u>82.0</u>	<u>75.1</u>	<b>71.5</b>	<u>58.1</u>	<u>40.7</u>	70.2	<b>57.8</b>	<u>43.6</u>	<b>26.5</b>	<b>34.0</b>	<b>68.25</b>	0.30

Table 14. Performance comparisons on VTAB-1k with ViT-B/16 models pre-trained on ImageNet-21K.

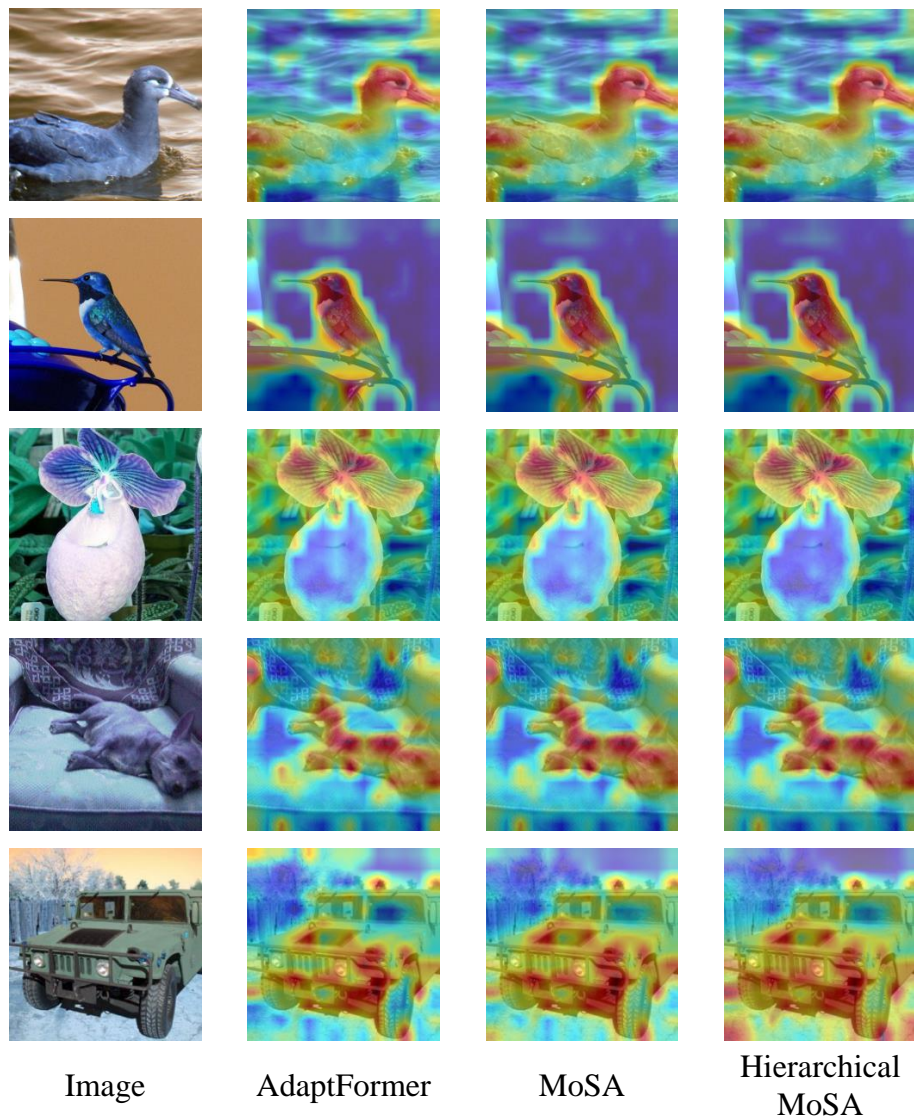


Figure 6. Attention map visualization on FGVC. From left to right: the RGB image, AdaptFormer, our MoSA and Hierarchical MoSA.

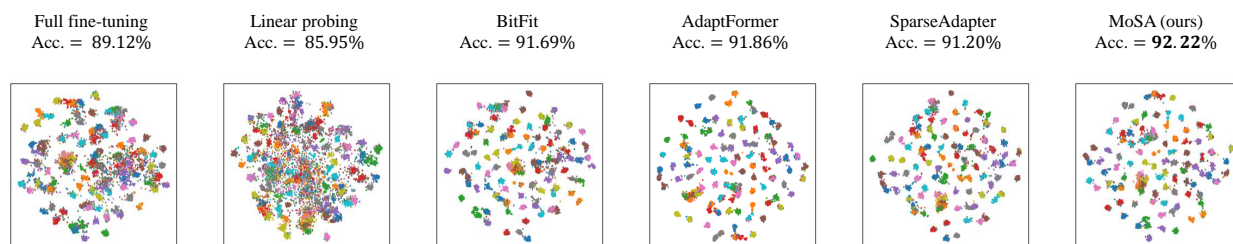


Figure 7. t-SNE visualization on CIFAR-100. From left to right: full fine-tuning, linear probing, BitFit, AdaptFormer, SparseAdapter and our MoSA (best viewed in color).